Distributed nerve gases sensor based on IR absorption in hollow optical fiber

R. Viola[a], N. Liberatore, D. Luciani*[a], S. Mengali [a], L. Pierno[b]
[a] Centro Ricerche Elettro Ottiche - via Pile 60, 67100 L'Aquila – Italy;
[b]Selex Sistemi Integrati SpA– via Tiburtina km 12.4, 00131 Rome – Italy

ABSTRACT

The Nerve gases are persistent gases that appear as very challenging menace in homeland security scenarios, due to the low pressure vapor at ambient temperature, and the very low lethal concentrations. A novel approach to the detection and identification of these very hazardous volatile compounds in large areas such as airports, underground stations, big events arenas, aimed to a high selectivity (Low false alarm probability), has been explored under the SENSEFIB Corporate Project of Finmeccanica S.p.A. The technical demonstrator under development within the Project is presented. It is based on distributed line sensors performing infrared absorption measurements to reveal even trace amounts of target compounds from the retrieval of their spectral fingerprint. The line sensor is essentially constituted by a widely tunable external cavity quantum cascade laser (EC-QCL), coupled to IR thermoelectrically cooled MCT fast detectors by means of a infrared hollow core fibers (HCF). The air is sampled through several micro-holes along the HCF, by means of a micropump, while the infrared radiation travels inside the fiber from the source to the detector, that are optically coupled with the opposite apertures of the HCF. The architecture of the sensor and its principle of operation, in order to cover large areas with a few line sensors instead of with a grid of many point sensors, are illustrated. The sensor is designed to use the HCF as an absorption cell, exploiting long path length and very small volume, (e.g fast response), at the same time. Furthermore the distributed sensor allows to cover large areas and/or not easily accessible locations, like air ducts, with a single line sensor by extending the HCF for several tens of meters. The main components implemented in the sensor are described, in particular: the EC-QCL source to span the spectral range of wavelength between 9.15um and 9.85um; and the hollow core fiber, exhibiting a suitably low optical loss in this spectral range (<1dB/m). Also, the characteristics of detectors and associated electronics for signal processing and data acquisition are discussed. Main results from preliminary measurements carried out are also presented.

Keywords: IR distributed sensors, absorption spectroscopy, quantum cascade lasers, hollow core fibers, nerve agents.

1. INTRODUCTION

Infrared absorption spectroscopy has been widely investigated and applied since decades for trace gases and vapors detection and identification[1]. New attention to this technique has been given in the last years, following the development of quantum cascade lasers, a novel powerful and compact solid state source, emitting in the spectral range of the medium infrared[2,3], that is the spectral fingerprint region for most of the targeted compounds in both military applications on battlefield and civilian applications of homeland security. A big effort has been devoted to the development of novel sensing devices allowing enhanced capability of detection in terms of both sensitivity and selectivity with reliable, small size and low power consuming sensors. A lot of academic and industrial R&D work has been carried out and it is still ongoing for prototyping and putting on the market new solutions[4]. Either point sensors, or remote sensor for standoff operation[5] have been proposed or are still under development to fulfill several operative requirements: large area coverage, very low limit of detection, identification capability, and fast response at once, also minimizing the probability of false positives and false negatives. In the field of homeland security the detection and identification of Nerve gases is one of the main investigation areas, because these gases not only can be lethal at very low concentrations (ppb level), but also their presence can be masked by typical urban gases, that can act as interferents since showing similar infrared absorptions[6,7]. An alternative approach to achieve distributed detection capability for homeland security, especially for indoor applications, has been investigated under the SENSEFIB Corporate Project of Finmeccanica S.p.A. and is presented hereafter.

Optics and Photonics for Counterterrorism and Crime Fighting VI and Optical Materials in Defence Systems Technology VII, edited by Colin Lewis, Douglas Burgess, Roberto Zamboni, François Kajzar, Emily M. Heckman,
Proc. of SPIE Vol. 7838, 78380H · © 2010 SPIE · CCC code: 0277-786X/10/$18 · doi: 10.1117/12.865009

2. SENSOR CONCEPT

The line-sensor concept is illustrated in Figure 1 below. An InfraRed source and detector are set at a distance of tens of meters, and coupled by an unrolled IR Hollow Fiber. A micro-pump sucks air into the fiber through an array of small, evenly distributed holes. With an internal core diameter of 0.5-1 mm, the hollow fiber opposes negligible resistance to the air flow, and the residence time of the air sample in the fiber is in the range of a few seconds. As such, the composition of the air sample in the fiber reflects continuously, accurately, and almost-real-time, the composition of the air around the fiber.

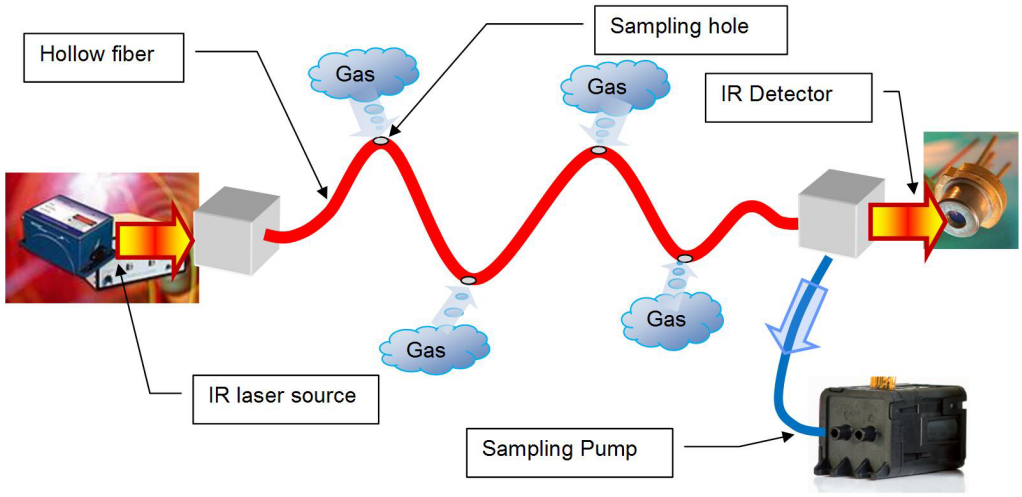

Figure 1 concept design of the line-sensor

The line-sensor concept appears particularly appealing whenever distributed chemical detection and identification capability is required over areas with strong spatial constraints, as is the case of public buildings, railway stations, airports, big stores, that are the typical targets of terroristic attacks. While narrow spaces severely limit the use of open-path and stand-off sensors, hollow-fibers can be laid to ground, cabled to walls, and adapted essentially to any site, to monitor streams of people and luggage, and even air ducts and venting pipelines, that are strategic for the security of crowded environments. Additionally, a limited number of line sensors can be used to replace a much larger number of point sensors and notwithstanding provide an adequate sampling and measurement grid. This will allow to reduce the number of sources and detectors, and therefore decrease the costs, while simplifying the installation and maintenance of the system. Noticeably, a grid of crossing line sensors may provide spatial resolution and locate the source of threat by cross-evaluation of measures from different sensors. The following Figure 2 illustrates the concept design of a small grid of line-sensors for indoor applications. The picture foresees the implementation of multiplexing devices and illustrates the possibility to increase spatial coverage and resolution of the grid by adding only hollow fibers. This means that different hollow fibers could be alternatively coupled to the same source/detector, or configured to switch the radiation and/or the air sampling on different paths, thus improving the grid, while retaining a minimal number of operating sources and detectors. The continuous operation is achievable thanks to the absence of cleaning and regeneration periods between successive measurements.

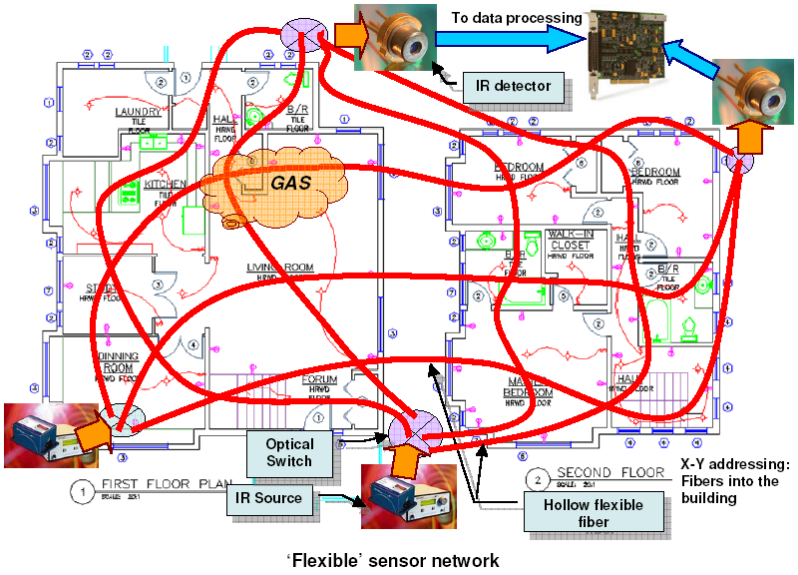

Figure 2 grid of line-sensors indoor applications

3. PRINCIPLE OF OPERATION

The line-sensor here proposed follows essentially the same functional scheme of most of the optical sensors based on spectroscopic absorption measurements. Here, new components combined with an original system architecture provide distributed detection capability with a single sensor. The detector measures the radiation emitted by the IR source after travelling through an absorption cell where it is partially absorbed by the target compound. In our sensor, the quantum cascade laser and the HCF are the IR source and the absorption cell, respectively. Absorption is wavelength dependent, and compound specific. It is described by the Lambert-Beer law as follows:

$$I(\lambda) = I_0(\lambda)\exp[-\alpha(\lambda)\, c\, l] \tag{1}$$

where $I_0(\lambda)$ and $I(\lambda)$ are the spectral radiation power intensities before and after traveling through the absorbing medium, $\alpha(\lambda)$ and c are the spectral absorption cross section and the concentration of the absorbing gas respectively; l is the optical absorption path length. The spectral absorbance $A(\lambda)$ is defined as:

$$A(\lambda) = \ln\left(\frac{I_0(\lambda)}{I(\lambda)}\right) \tag{2}$$

By comparing (1) and (2) the following expression of the spectral absorbance can be derived:

$$A(\lambda) = \alpha(\lambda)\, c\, l \tag{3}$$

It is proportional to gas concentration and spectral cross section and can be conveniently used for absorption measurements. Both trace detection and identification capability can be achieved by measuring $A(\lambda)$ in the so called 'fingerprint spectral region' of medium infrared (MIR), where most hazardous compounds exhibit their strongest and compound-specific absorption cross sections.

3.1 Limit of detection (LoD) as a function of the fiber length

Equation (1) is valid if neglecting transmission losses due to the optical cell. Neglecting from now on the spectral dependence on wavelength explicitly, if we now consider a hollow fiber with a transmission loss coefficient α_f, the equation (1) must be replaced by:

$$I = I_0 \exp(-\alpha\, c\, l)\exp(-\alpha_f l) \tag{4}$$

The limit of detection of the sensor can be defined as the condition for which the gas induces a signal variation equal to the noise N of the system:

$$|\Delta I|_{LoD} = N \tag{5}$$

For small concentration the absolute value of the signal variation due to the absorption of a gas inside the fiber can be derived from (4) and expressed as:

$$|\Delta I| = I_0\ \alpha\, c\, l \exp(-\alpha_f l) \tag{6}$$

Substituting (5) in (6) and resolving respect to c it is possible to retrieve the minimum detectable concentration:

$$C_{LoD} = \frac{N \exp(\alpha_f l)}{I_0 \alpha\, l} \tag{7}$$

The minimum detectable concentration C_{LoD} is intuitively proportional to N/I_0, and inversely proportional to α (and is therefore compound- and wavelength-specific). Furthermore, if we assume that the system noise N is not dependent on the length of the fiber, by deriving (7) respect to the fiber length l we find that C_{LoD} reaches a minimum for $l = 1/\alpha_f$. This is shown in Figure 3, where limits of detection are drawn, for different values of the fiber transmission loss, as a function of fiber length. In the figure C_{LoD} has been calculated by setting arbitrarily the constant value of $N/I_0\alpha$ equal to 1. For practical applications, hollow fibers with an attenuation loss of 1 dB/m appear suitable to cover distances up to around 20-30 m, while fibers with attenuation of 0.5 dB/m could be used for lengths of 50-60 m and beyond.

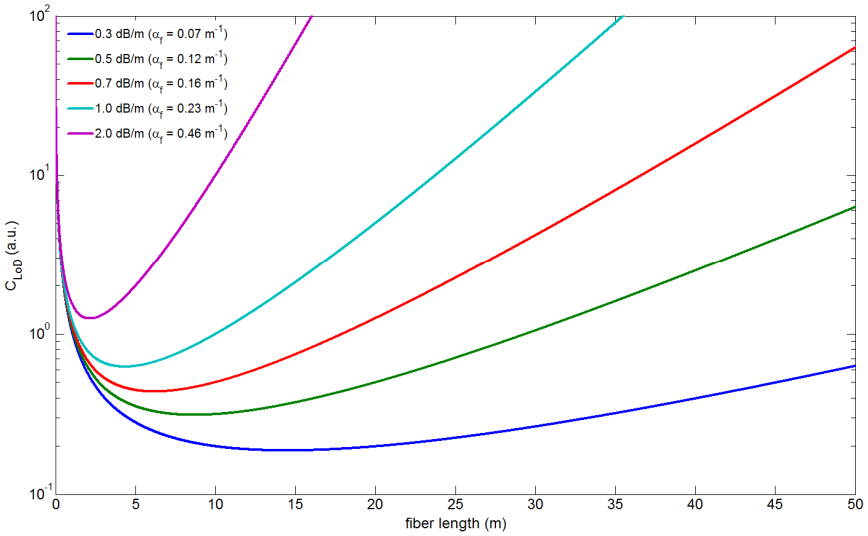

Figure 3 LoD as a function of the length of the HCF and for different values of the fiber transmission loss.

Quantum cascade lasers can emit high spectral power intensity in the MIR, allowing the implementation of HCF to achieve long absorption path (e.g. trace sensitivity) and fast response at the same time. If extending the HCF and sampling the air by means of micro-holes, properly distributed all along the fiber, it is possible to cover extended areas with a single line sensor, that is by means of a single laser source and a single IR detector. The principle of operation of a single line-sensor is still applicable to a grid of line-sensors in order to assess measurement capability over extended areas, also adding capability to retrieve the location of the threat by means of cross detection from different line-sensors.

4. SYSTEM ARCHITECTURE

A possible architecture of the line-sensor, as it has been designed and implemented in our sensor, is illustrated in the following Figure 4.

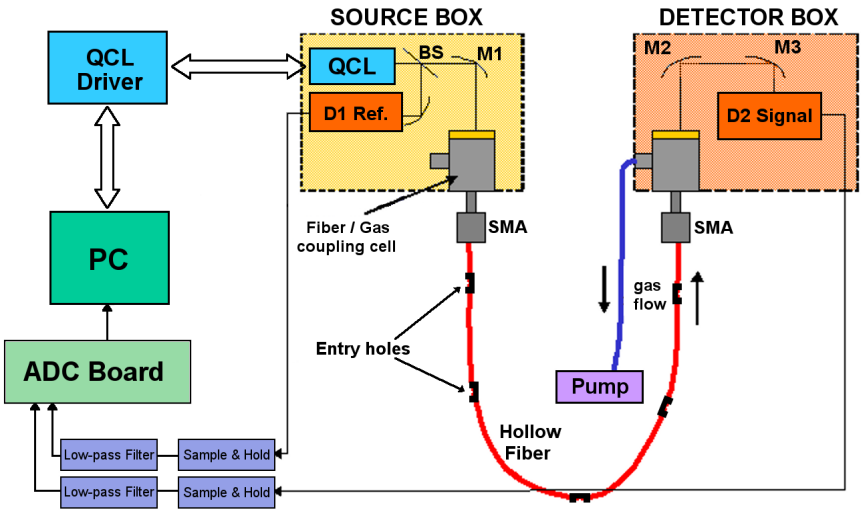

Figure 4: block diagram of the sensor architecture showing main components and interfaces

In the design of the system illustrated in Figure 4, an external cavity quantum cascade laser has been considered to take advantage of the measurement capability over an extended spectral range, in order to perform identification of targeted compounds. The laser beam is injected inside the HCF by means of appropriate optical couplings, after splitting the beam to have a reference signal of the source emission for normalization. In order to assure minimal loss of energy in our system, off-axis parabolic mirrors of appropriate focal length have been selected to focalize the laser beam within the hollow core of the fiber, also minimizing the angular aperture of the focusing beam, that translates into a better transmission efficiency of the HCF. After traveling inside the hollow core fiber, the radiation exits from the end side of the fiber and it is focused onto the detector. Other key elements of the system, as they are shown in the picture, are two opto-mechanical couplers, each one at one end of the HCF. They allow both the infrared radiation to travel in and out of the HCF, by means of appropriate optical windows, and the air under sampling to be flushed in and out of the fiber by means of suitable fittings toward the sampling micro pump. These two couplers have been designed to achieve minimal internal volume, in order to assure the total exchange of air sampled inside the fiber in a very short time. A PC control unit is interfaced both with the external controller of the laser head and with the electronics of the IR receiver to run the sensor and manage the signal processing and data acquisition.

5. EXPERIMENTAL SET UP

As mentioned above, the main parts that characterize the line-sensor are: the EC-QCL source and the HCF. Then, IR detectors, several optical and opto-mechanical couplings, and appropriate electronics complete the system. In the following, the main characteristics of the several components of the line-sensor are described.

5.1 EC-QCL

The laser source implemented is a commercially available external cavity tunable quantum cascade laser from Dayligth Solutions. The laser emission can be tuned within the spectral range of wavelength between 9.13 μm and 9.87 μm, by means of a miniaturized external grating that is integrated inside the optical head of the laser. It can be used both in pulse operation, with a maximum duty cycle of 5 %, or with a continuous emission, but in this case it needs an external chiller. Altough the scan resolution is of 0.1 cm-1, in pulse mode itis ultimately limited by the laser line width of 1 cm-1. Main specifications of the laser are reported in table 1.

Table 1: EC-QCL specifications

Spectral scan	9.15-9.85um
Scan resolution	0.1cm^{-1}
Peak pulsed power	200mW
PRF	100Hz-100KHz
Pulse duration	40-500ns
Max duty cycle	5%
Line width	1cm^{-1}
Beam divergence	<5mrad

5.2 IR HCF

Hollow core IR waveguides[8] were developed mainly for transmission of high power CO2 laser beams, to be used, for example, in medical and surgical applications. Since radiation is confined inside the hollow core of the waveguides, they can withstand high power density without damaging effects on the waveguide cladding. Both the wavelength peak transmission and the whole spectral range of operation are determined by the design of the inner reflective layers.

The hollow core fiber implemented in our sensor is of single dielectric/metallic layer type, from Polymicro Technologies. The structure of the fiber is illustrated in Figure 5. The capillary tube is made of fused silica. For protection, it is coated with an external jacket of acrylate, which improves the strength and flexibility of the fiber. The

internal reflective coating has the peak transmission around 10.6um, (CO2 laser emission), but it is suitable to be utilized in the whole spectral range of emission of the EC-QCL of our sensor, with transmission losses of less than 1dB/m along the fiber. This was verified by measuring the spectral transmission loss of the HCF by means of the same EC-QCL. Results are reported in Figure 5.

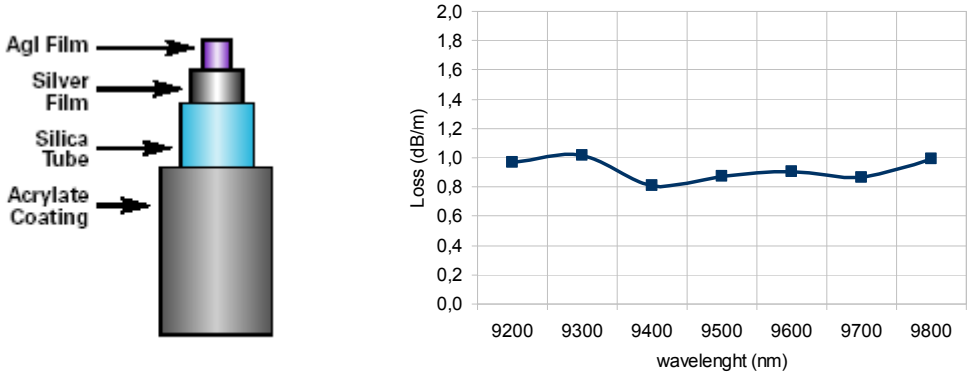

Figure 5: structure of the HCF (on the left); measured spectral transmission loss of the HCF (on the right)

In Figure 6 it is shown the result of a preliminary attempt to make micro holes across the cladding of the HCF in order to fill it with the surrounding air inspired by means of the micro pump connected to one end side of the HCF. The holes have been made by means of high power CO2 laser shots. In the picture on the right, showing a cross section of the HCF, the final shape of the hole, as it appears crossing through both the inner silica capillary and the protective external acrylate buffer of the HCF, it is illustrated.

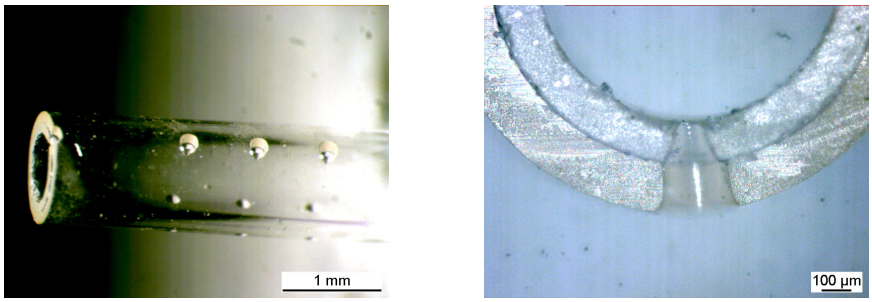

Figure 6: images of the micro holes obtained by means of laser drilling showing some micro holes along the HCF (on the left), and the cross section of one micro hole across the fiber (on the right).

Since the drilling process produces defects inside the internal reflective wall of the hollow core, the transmission efficiency of the HCF, before and after drilling, has been measured to assess degradation. By comparing the transmittance of unaltered HCF with the transmittance of perforated HCF of the same length, about 0.5 dB loss for each hole has been estimated.

5.3 TEC MCT detectors

As mentioned previously, the beam of infrared radiation emitted by the laser source is split before entering into the HCF to normalize measurements with a reference signal of the laser emission power. Two equal detectors are used to acquire both the reference signal before the fiber and the signal as it is emerging from the exit aperture of the HCF. They are

mercury cadmium telluride photoconductive detectors. The packaged detectors can be operated at room temperature. The main characteristics of these detectors are reported in table 3. Owing to the very fast response of the detectors (rise time <3ns), the detectors are suitable to acquire and integrate measurements on a shot by shot basis when operating the laser in pulsed mode and at its maximum pulse repetition frequency (PRF) of 100 KHz.

Table 3: TEC MCT specifications	
Detector material	HgCdTe
Cooling temperature	265K
Spectral response	4-12um
Responsivity	2500V/W
Detectivity	$>2.5x10^{9}cmHz^{1/2}W^{-1}$
Active area	1mmx1mm
Rise time	<3ns
Power consumption	<3W
Room temperature operation	

5.4 Opto-mechanical interfaces

The experimental set up is completed with several optical and opto-mechanical couplings. Standard items, when available from the market, have been selected for implementation. Other key components have been purposely designed to maximize the throughput efficiency of the line-sensor, also considering the dual functionality of the HCF for acting as the optical absorption cell of the sensor, and also to bring the air under sampling inside and outside of the hollow core of the fiber. Off-axis parabolic mirrors have been selected for the optical coupling of the HCF endings with the laser source and detectors. They allow to inject the laser into the HCF and to collect the radiation going out the exit aperture of the fiber matching the core diameter of the HCF with the laser beam size and divergence on one side, and with the detectors active area on the other side. The opto-mechanical subsystems, as assembled to interface the HCF with the laser source and with the IR detector for prototyping of the line-sensor, are shown in the following Figure 7.

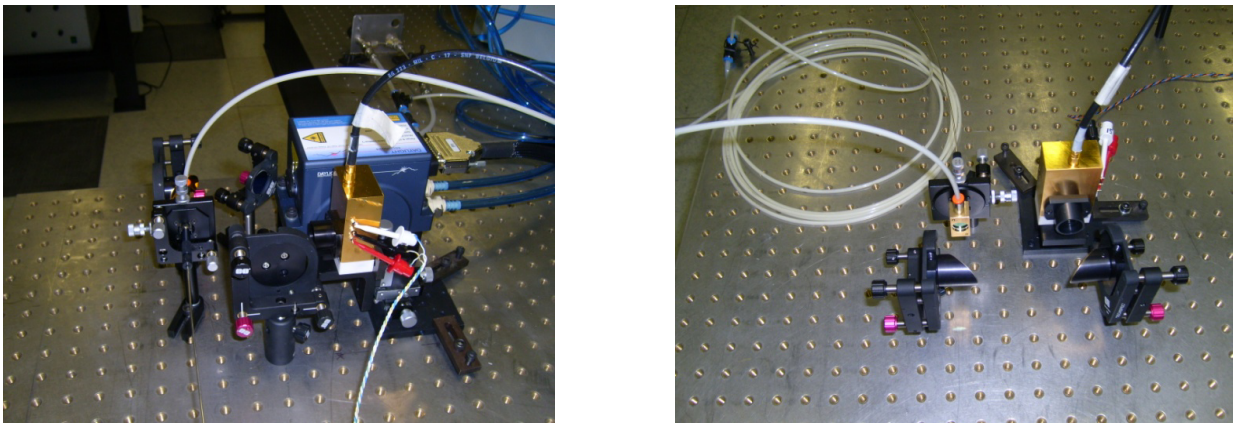

Figure 7: pictures of the laboratory set up showing the opto-mechanical sub assemblies of the line-sensor for interfacing the laser source with the inlet of the HCF and with the detector for reference (on the left), and to interface the outlet of the HCF with the other IR detector (on the right).

As mentioned above, the non standard components of these opto-mechanical interfaces are the two micro cells that allows both the IR radiation and the air sampled to enter inside and exit from the HCF. They have been specifically designed and realized, in order to minimize the overall internal volume of the sensor where the air sampling takes place, in order to speed up the exchange of air inside the HCF avoiding dead volumes. This will affect the sensor performance, mainly in terms of time of response. In fact, higher internal volume translates into longer times to replace completely the

air sampled inside the HCF. The dual functionality of this interfaces is illustrated in Figure 8, where a 3D layout of the micro cell cross section is illustrated. It shows how the IR laser radiation and the air under sampling can pass through a common path inside the HCF, while they are separated outside of the HCF, to allow air sampling and radiation measurement simultaneously.

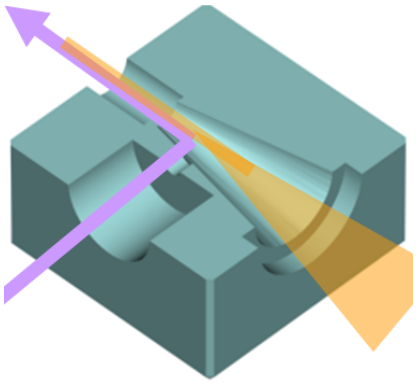

Figure 8: 3D layout illustrating a cross section of the cell for interfacing the HCF with the IR source/detector and the air sampling circuit.

5.5 Electronics

The electronics implemented in the acquisition chain of the sensor is schematically reported in Figure 9.

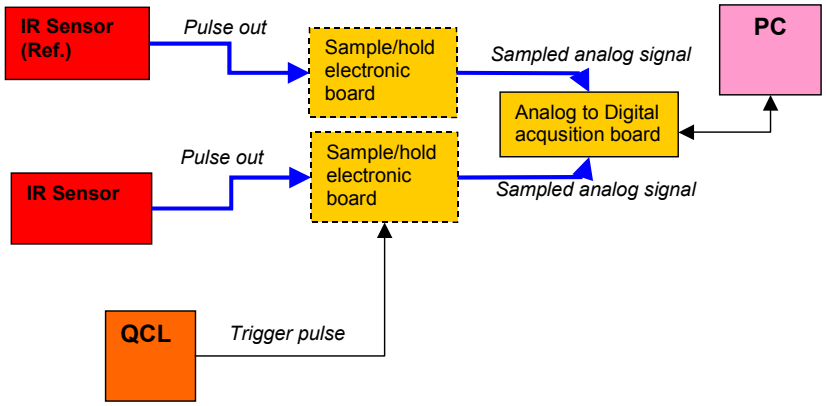

Figure 9: schematics of the electronics

Operating the laser in pulsed mode, the signals coming out from both the signal and reference fast detectors, are short pulse of less than 500nsec. In order to avoid a very high speed sampling (to reconstruct the pulse) the pulses are sampled with monolithic sample/hold amplifiers. They acquire the signal value and maintain that value during the pulse time. With this architecture a lower sampling speed, with high resolution on the signal amplitude can be achieved. A PC unit controls both the laser head of emission, by means of the external laser controller, and the synchronous acquisition of signals measured by the two detectors, by means of the two sample&hold and the ADC board. The reference signal from the source and the signal coming out from the fiber are both acquired to suppress fluctuations due to the source, in order to extract spectral absorption features respect to the background.

6. RESULTS AND DISCUSSION

This section reports initial results from early measurements with the experimental set up described before. These results, although preliminary, allow to evaluate the potential sensor performance in terms of detection and identification capability through meaningful examples. Although the sensor is intended for Chemical Agents, these tests have been carried out with Vapour Organic Compounds, for safety and security reasons. VOCs have been selected in consideration of their spectral absorption affinity with nerve agents. The IR absorption spectra of isopropyl alcohol, both as measured and as retrieved from the PNNL database[9], are shown in Figure 10. The IR absorption spectrum of sarin in the same spectral range is given in Figure 11. Absorption features are similar, although positioned at different wavelength. It is worth to note that when dealing with low concentrations of target compounds, absorptions are proportional to the concentration and to the spectral absorption cross section. Thus, results obtained with simulants can be easily scaled to infer with reasonable accuracy the performance we can expect with Chemical Agents.

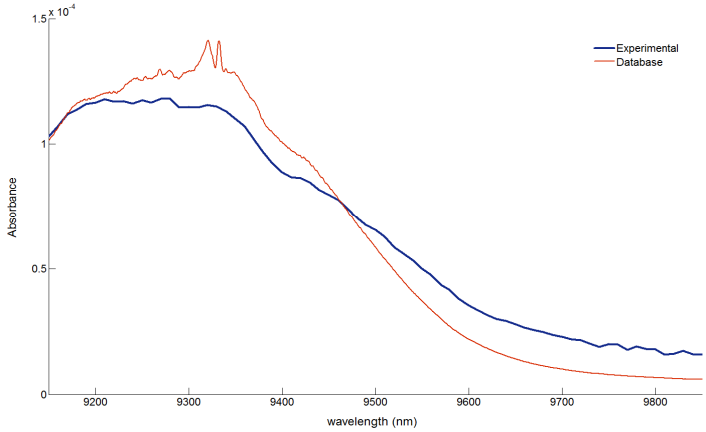

Figure 10: IR absorption spectrum of isopropyl alcohol, as measured (blue curve), and as retrieved from database (red curve). The plot scale for absorbance refers to the curve from database, corresponding to 1ppm-m of concentration. The experimental curve was obtained with saturated vapors at room temperature and it has been rescaled for comparison.

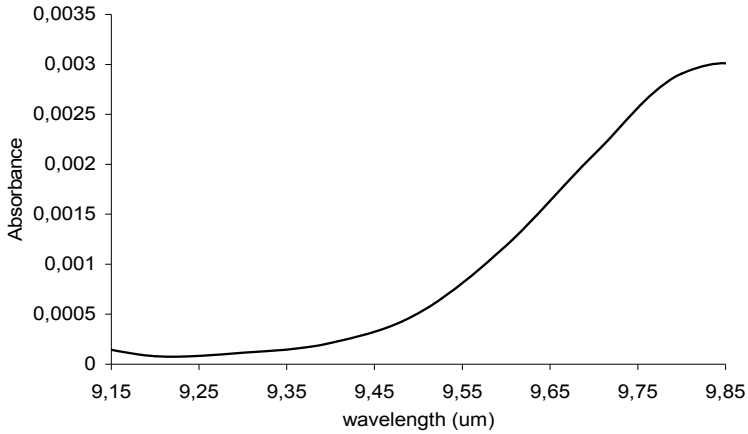

Figure 11: IR absorption spectrum of Sarin in the same spectral range considered in Figure 10 for isopropyl alcohol.

The response time of the sensor is limited by the time spent by the laser source to execute the spectral scan. A complete spectrum can be acquired through a single scan in less than one second. Nonetheless, better results are obtained by

integrating measurements from multiple scans, so increasing the signal to noise ratio and consequently improving the limit of detection. Anyway, the final response time should be traded off against the limit of detection that is required. Figure 12 shows the IR absorption spectrum of ethyl alcohol measured by our line-sensor and integrated over 14 spectral scans. The spectrum was obtained with a 2m long HCF, by sampling the vapour through six holes equally spaced along the fiber. In the figure, the reference spectrum from the PNNL database is rescaled to the concentration that matches the measured spectrum. A very good spectral matching can be observed. A small shift that slightly grows with wavelength can be observed between corresponding peaks in the two spectra. It should be due to the application of uncorrected reference of wavelength vs. scan time for the measured spectrum, because the spectral scan was not calibrated before this preliminary measurements. The concentration applied to rescale the spectrum from database can be considered as a good estimate of the measured concentration. In this case a measured concentration of around 200ppm of ethyl alcohol can be estimated.

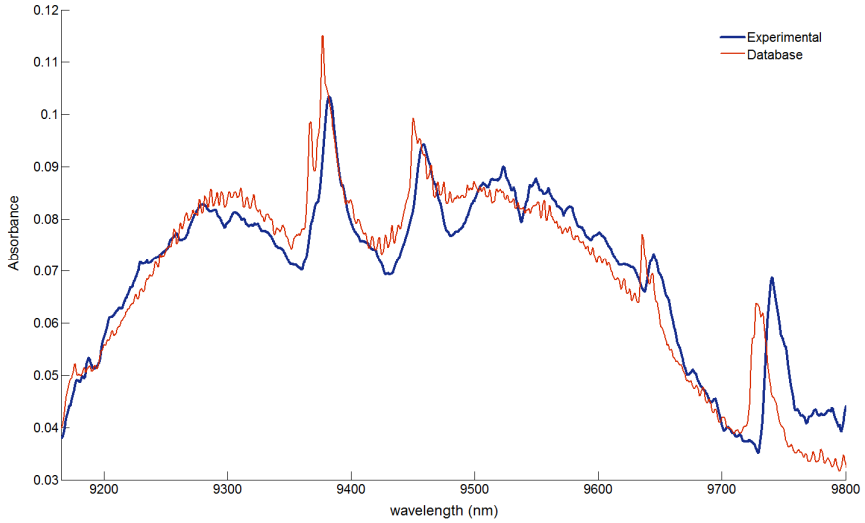

Figure 12: Comparison between the IR absorption spectrum of ethyl alcohol, as obtained by integrating 14 spectral scans, and the corresponding IR spectrum retrieved from the PNNL database.

Different strategies of digital sampling for signal acquisition, and several algorithms for signal processing are under investigation, aiming at maximizing S/N and improving the identification capability of the sensor. In any case, by taking the S/N values available at fixed wavelengths, we are already able to estimate limits of detection of Chemical Agents at those wavelengths.

6.1 Limit of Detection

Limits of detections can be estimated by replacing in equation (7) the experimental signal to noise ratio measured at the output of the fiber:

$$\frac{S}{N} = \frac{I_0 \cdot \exp\left(-\alpha_f l\right)}{N} \tag{8}$$

Some estimates are reported in the following table. The average signal to noise ratios have been calculated considering the noise over 40 seconds and integrating signals over 1 second. Results are reported for three wavelengths indicated in the first column. Signal to noise ratios are reported in the 2nd column. The absorbance of 1 ppm of Sarin for an absorption path of 1m is indicated in the 3rd column. The detectable amounts of Sarin, i.e. the minimum amount of Sarin

that provides an absorbance at the same wavelength equal to the minimum measurable absorbance is reported in the last column.

Table 4. Signals to noise ratio and limit of detection at fixed wavelengths.

Wavelength (nm)	**S/N**	**Sarin spectral Absorbance @1ppm-m**	**C_{LoD} for Sarin (ppb)**
9300	3096	$2.29 \cdot 10^{-4}$	829
9450	9375	$5.07 \cdot 10^{-4}$	123
9700	3076	$4.37 \cdot 10^{-3}$	44

ACNOWLEDGEMENTS

This work was supported by Finmeccanica SpA under the Corporate Project SENSEFIB. Thanks are due to Giovanni Farina and Alberto Germagnoli, from the Linkra Microtech Division of Linkra s.r.l., for drilling of the HCF.

REFERENCES

[1] R. F. Curl and F. K. Tittel, "Tunable infrared laser spectroscopy", Annu. Rep. Prog. Chem., Sect. C, 2002, 98, 219–272.
[2] A.A. Kosterev, F.K. Tittel, "Chemical Sensors Based on Quantum Cascade Lasers", IEEE J. Quantum Electron. (Spec. Issue Quantum Cascade Lasers) 38, 582 (2002)
[3] A.Kosterev,G.Wysocki,Y. Bakhirkin, S. So, R. Lewicki, M. Fraser, F. Tittel, R.F. Curl, "Application of quantum cascade lasers to trace gas analysis", Applied Physics B: Lasers and Optics 90 (2008) 165–176.
[4] E. Normand, I. Howieson, M. McCulloch, P. Black, "Quantum Cascade Laser (QCL) based sensor for the detection of explosive compounds", Proc. of SPIE Vol. 6402, 64020G, (2006).
[5] E. B. Takeuchi, T. Rayner, M. Weida, S. Crivello, T. Day, "Standoff detection of explosives and chemical agents using broadly tuned external-cavity quantum cascade lasers (EC-QCLs)", Proc. of SPIE Vol. 6741, (2007).
[6] M. E. Webber, M. Pushkarsky, C. Kumar, N. Patel, "Optical detection of chemical warfare agents and toxic industrial chemicals: Simulation", J. Appl. Phys. 97, 113101 (2005).
[7] M. Pushkarsky, M. E. Webber, T. Macdonald ,C. Kumar, N. Patel, "High-sensitivity, high-selectivity detection of chemical warfare agents", Appl. Phys. Lett. 88, 044103 (2006).
[8] J. A. Harrington, "A Review of IR Transmitting, Hollow Fibers", Fiber and Integrated Optics, 19, 211-217 (2000).
[9] Pacific Northwest National Lab (PNNL) database of IR absorption spectra: https://secure2.pnl.gov/nsd/nsd.nsf/Welcome .